has been plotted as a function of the neutron number of the iodine member. For masses 126–132 the Q_{β^-} values listed in the table of Strominger, Hollander, and Seaborg[14] have been used. The value for mass 134 is taken from Cameron's table of mass excesses and decay energies,[15] and that for 136 is from the present work. These data emphasize the discontinuity in decay energy associated with the closing of the 82-neutron shell.

[14] Strominger, Hollander, and Seaborg, Revs. Modern Phys. **30**, 585–904 (1958).
[15] A. G. W. Cameron, Atomic Energy of Canada Limited, Report CRP-690, 1957 (unpublished).

ACKNOWLEDGMENTS

The authors would like to express their appreciation to E. Eichler, J. T. Wasson, and J. W. Chase for their assistance in several phases of the experiments, and to Dr. Eichler and Dr. G. Scharff-Goldhaber for their helpful criticism of the manuscript.

PHYSICAL REVIEW VOLUME 114, NUMBER 1 APRIL 1, 1959

Cloud-Chamber Measurement of the Half-Life of the Neutron*

N. D'ANGELO
Argonne National Laboratory, Lemont, Illinois
(Received November 3, 1958)

The half-life of the free neutron has been measured by a cloud-chamber method. It turned out to be 12.7 min with an error of ~15%, ~10% being due to the poor statistics. This determination has about the same accuracy as the best previous measurement and confirms it by an independent method.

I. INTRODUCTION

THE beta decay of the neutron, which was first predicted by Chadwick and Goldhaber,[1] was observed by Snell and Miller[2] in a neutron beam from the Oak Ridge pile. Snell, Pleasanton, and McCord[3] detected coincidences between electrons and low-energy positive particles of approximately the mass of the proton. By a spectrometer method, Robson[4–6] showed the positive particles to be protons and was able to get the energy distribution of the electrons. He found the half-life for neutron decay to be 12.8 minutes, with an error of ±2.5 minutes. The problem was also taken up by Spivak *et al.*[7] Their first measurements gave the half-life in the range 8–15 minutes. The accuracy was then increased and a half-life of 12±1.5 minutes was obtained. In all the above measurements, the products of the decay were detected by means of counters. Protons were accelerated by electrostatic fields and the errors were due mainly to the uncertainty in the value of the collection factor.

It seemed then of some interest to repeat the measurement of the neutron half-life by using a completely different method and trying to eliminate the uncertainty introduced by the collection factor. The idea of the experiment described in this paper is the following. (See Fig. 1.) A neutron beam from the Argonne CP-5 reactor is freed from gamma rays and is sent through the sensitive region of a diffusion chamber where the events occurring are photographed at a rate of, say, two frames per second. The number of recorded electrons which can be attributed to neutron decays should give the half-life when the neutron density in the chamber is known from activation measurements.

No problems should arise in finding the collection factor of the decay products. On the other hand, background problems more serious than those faced by other authors have to be overcome. All the possible sources of background electrons have to be reduced to an acceptable level. They are expected to come mainly from (1) gamma rays from the room background, (2) gamma rays in the neutron beam, and (3) gamma rays produced by neutron captures in the walls of the cloud chamber or in the surrounding materials.

A heavy lead housing shields the cloud chamber and a neutron mirror reduces the gamma rays in the beam to a tolerable level. Materials with low absorption cross section for thermal neutrons are used in the construction of the cloud chamber. Very thin Mylar windows at the entrance and exit of the neutron beam from the chamber also reduce the electron background caused by (3).

In the following sections we shall describe (a) the diffusion chamber, (b) the method of obtaining a suitable beam, (c) the shielding of the chamber, (d) the operation of the chamber, (e) the experimental results, and (f) the conclusions.

* Work performed under the auspices of the U. S. Atomic Energy Commission.
[1] J. Chadwick and M. Goldhaber, Proc. Roy. Soc. (London) **A151**, 479 (1935).
[2] A. H. Snell and L. C. Miller, Phys. Rev. **74**, 1217 (A) (1948).
[3] Snell, Pleasanton, and McCord, Phys. Rev. **78**, 310 (1950).
[4] J. M. Robson, Phys. Rev. **77**, 747 (1950).
[5] J. M. Robson, Phys. Rev. **78**, 311 (1950).
[6] J. M. Robson, Phys. Rev. **83**, 349 (1951).
[7] Spivak, Sosnovsky, Prokofiev, and Sokolov, *Proceedings of the International Conference on the Peaceful Uses of Atomic Energy, Geneva*, 1955 (United Nations, New York, 1956), Paper No. 650.

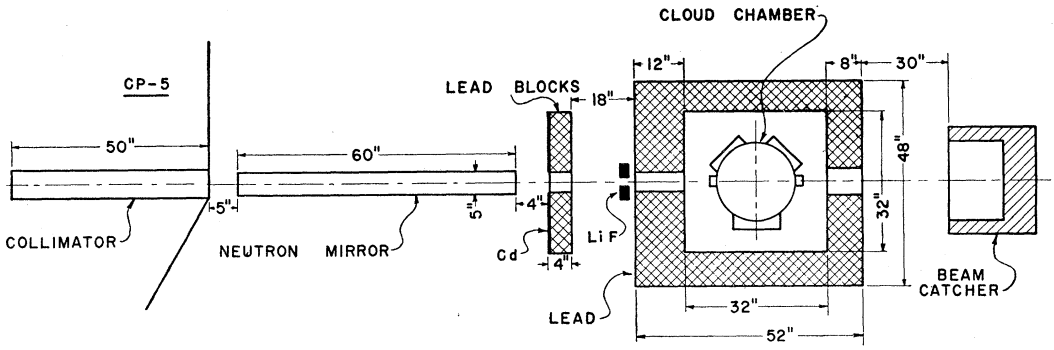

FIG. 1. General arrangement (not to scale).

II. THE DIFFUSION CHAMBER

The chamber works by downward diffusion of methyl alcohol vapor in a mixture of oxygen ($\sim\frac{1}{2}$ atmos) and helium ($\sim\frac{1}{2}$ atmos), from a warm region (at about 35°C) to a horizontal cold surface (at about −60°C) which is cooled by a flow of acetone circulating through a heat exchanger in a mixture of acetone and dry ice. Near the cold surface a continuously sensitive layer ~2 inches deep is obtained. Tracks are photographed through the top window of the chamber.

The diffusion chamber is built of 61-S aluminum alloy and consists of three main parts (Fig. 2): (1) the bottom with its cooling coils, (2) the cylindrical body with the windows for the illumination and for the neutron beam, and (3) the conical region, with the methyl alcohol source and coils for circulation of warm water.

The bottom is made of two circular plates, in one of which is milled a system of circular grooves. The two plates are welded together at the periphery to obtain a system of spiral channels in parallel to be used to circulate the refrigerating acetone. Two chanels in parallel, instead of one, are used to get a more uniform temperature distribution on the bottom of the chamber in order to avoid any effects (such as turbulent motions, radial gas currents, etc.) which could arise if the temperature distribution were too nonuniform.

The cylindrical body of the chamber is of aluminum $\frac{3}{8}$ in. thick. The neutron beam enters and leaves the chamber through Mylar windows about 2 mils thick. The length of the two arms with the Mylar windows is approximately 3 inches. The chamber has three windows for illumination, the large one for continuous illumination for visual observation and the other two for the flashes used in the photography.

The cylindrical body is insulated from the conical section by a micarta ring. The screws fastening the sections together are provided with insulating micarta rings to provide electrical insulation between the top and the bottom of the chamber so that an electric sweeping field may be applied. Black velvet covered with a very thin glass plate on the bottom of the chamber provides the background for the photography.

The sensitive region is insulated from the outside walls by a polystyrene cylinder $\frac{1}{4}$ inch thick, about 4 inches high, and slightly smaller in diameter than the cylindrical body. In addition, a tape heater wrapped around the top of this cylinder (just below the level of the micarta ring) provides the right temperature distribution along the boundary of the sensitive region. This inner cylinder has two openings for passage of the neutron beam. To prevent turbulent motions of the gas and the vapor, these openings are closed with Mylar sheets $\sim\frac{1}{2}$ mil thick.

The events occurring in the chamber are photographed with a Varitron Beattie Camera, Model DR-2. The light for a photograph is provided by charging a 200-μf bank of condensers to 1500 volts and discharging them through two linear G.E. Model FT-126 flash tubes. Fairly well collimated beams of light are obtained by using cylindrical Lucite lenses. The film used is Kodak Tri-X. The camera lens is a Baltar, 50 mm, f/2.3, of the Bausch & Lomb Optical Company.

Stereoscopic pictures of the events occurring in the chamber are taken at a rate of two frames per sec. A beam splitter and a single camera are used to get two pictures (on the same frame) of the particular event to be recorded. Then an ordinary projector projects the pictures on a screen where the distance is measured between the two points corresponding to the same point of the recorded track. From this distance one can deduce the height of this point relative to the bottom of the chamber. For further details about the chamber and the photographic system, see the report by Caglioti and D'Angelo.[8] Remarks on the operation of the chamber will be given in Sec. V.

III. THE NEUTRON BEAM

The requirements the neutron beam has to satisfy are that it must have (*a*) high neutron density, (*b*) very low gamma background, and (*c*) good collimation and small vertical spread. Since there is no need for the neutrons to be monoenergetic, a neutron mirror seemed

[8] G. Caglioti and N. D'Angelo, Argonne National Laboratory, Report ANL-5745, June, 1957 (unpublished).

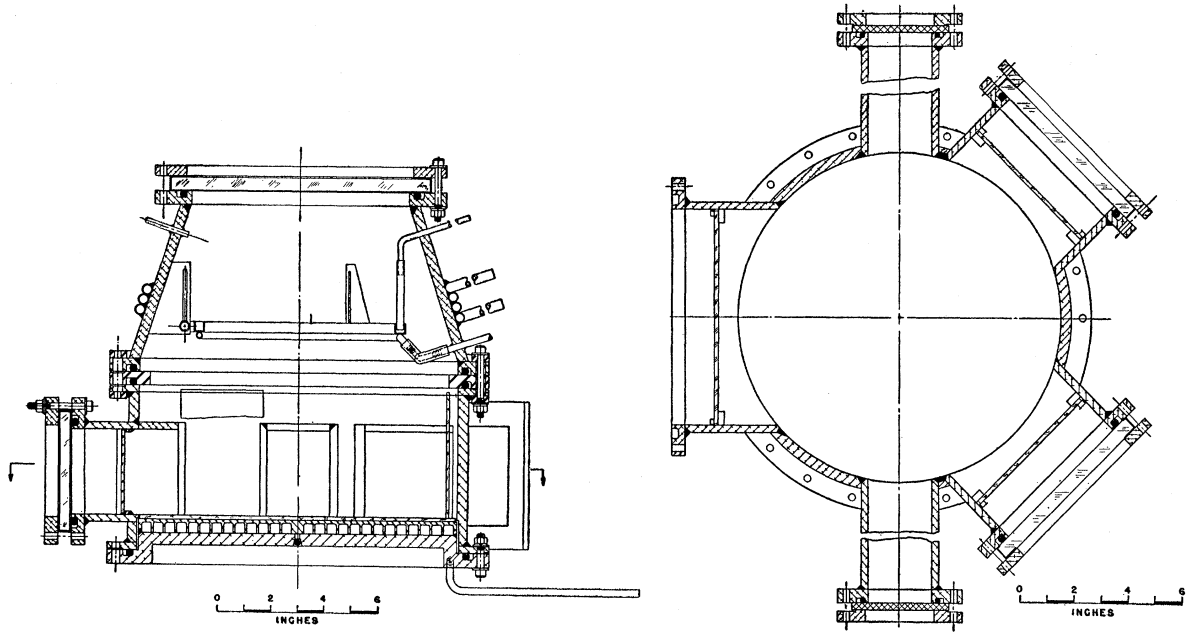

FIG. 2. The diffusion chamber.

to be the best means of achieving requirements (*a*), (*b*), and (*c*).

The neutron beam incident on the mirror is collimated by a brass collimator ~50 inches long, with a rectangular slit 4 inches wide by $\frac{1}{8}$ inch high. Before the neutron mirror was put in place, the neutron beam emerging from this collimator was mapped with a neutron counter whose sensitive area was a circle $\frac{5}{32}$ inch in diameter. The neutron counter was 75 inches from the pile face. A graphite plug 12 inches long was inserted in the beam hole all the way down into the graphite reflector of the pile and was left there throughout all the subsequent measurements. The result of a vertical scanning of the beam is shown in Fig. 3, in which the counting rate is plotted against the number of turns of the screw which determines the vertical position of the counter. Ten turns of the screw correspond to a 1-inch vertical displacement of the counter. The neutron flux 75 inches from the pile face and in the center of the beam turned out to be about 8×10^6 neutrons cm^{-2} sec^{-1}. After these preliminary measurements, the mirror was put in place.

The mirror was made of nickel since this element has one of the highest values of Na, where N is the number of nuclei per unit volume and a is the scattering length. Hence, other things being equal, a nickel mirror would give a good separation between the reflected beam and the undeviated beam. The mirror consists of five plates, each 1 foot$\times$5 inches$\times\frac{1}{2}$ inch, laid in a row along the direction of the beam. The top surface of each plate was optically worked to flatness within a few fringes over a width of 2 to 3 inches. These plates were supported by a horizontal steel plate which can be displaced vertically by means of three adjusting screws having 20 threads per inch. Two of these three adjusting screws were on the end placed only a few inches from the pile face.

To obtain the maximum flux of reflected neutrons, the mirror was first kept horizontal while its height was increased until the mirror started to intercept the beam. The positions of the two screws near the pile face then were fixed, and the beam was scanned again for various positions of the third screw. Figure 4 shows the result of one of the scannings with the counter 132 inches from the pile face. At this position, the neutron flux in the direct beam had turned out to be about 6×10^6 neutrons cm^{-2} sec^{-1}. In the reflected beam, when the mirror was set up as in Fig. 4, it turned out to be about $\frac{1}{6}$ of that in the direct beam. The gamma background in the direct beam at 132 inches from the pile face was ~10 r/hr. At the same distance in the reflected beam it turned out to be of the order of 10 mr/hr.

In an attempt to lower the gamma background and

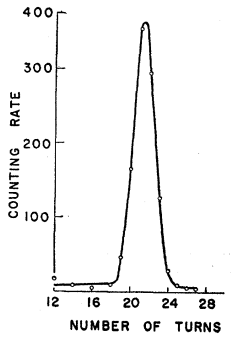

FIG. 3. Vertical distribution of neutrons in the direct beam at ~75 in. from the pile face.

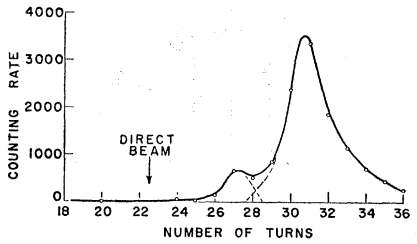

FIG. 4. Reflected beam at ~132 in. from the pile face.

thereby increase the signal-to-noise ratio for the electrons produced in the cloud chamber, the collimator opening was narrowed from $\frac{1}{8}$ inch to $\frac{1}{16}$ inch. However, the reduction of neutron flux was at least as great as the reduction of background so the net effect was slightly detrimental. Hence the width was kept at $\frac{1}{8}$ inch.

A better procedure was found to be the following. A lead plate 5 inches wide, 6 inches long, and $\frac{1}{4}$ inch thick was set immediately after the last nickel plate on the steel plate supporting the mirror, and protruding slightly above the plane of the mirror. The position of the lead plate could be adjusted by means of four regulating screws so as to get rid of the last gamma rays still present at the very end of the tail of the direct beam without greatly decreasing the intensity of the reflected beam (Fig. 5). A steel plate, 5 ft×6 in.×$\frac{3}{8}$ in., was put about $\frac{3}{8}$ in. above the nickel mirror and parallel to it to reduce the general gamma background. Mirror and steel plate were then completely surrounded with Cd sheets to cut off the neutrons scattered (not reflected) by the mirror. Cd was particularly necessary at the end of the mirror facing the cloud chamber. Only a very narrow (~$\frac{3}{8}$ in.) slit was left open to allow the reflected beam to go through. A Bi absorber 2 inches thick was placed between the pile face and the mirror.

The chamber was set up so as to have the neutron beam crossing the sensitive region approximately 1 inch above the bottom. The lead shielding of the chamber was then added, as will be described in Sec. IV. The beam is further collimated by passing through a $\frac{7}{8}$ in.×$\frac{3}{8}$ in. rectangular hole through ~1 inch of LiF powder packed in a hard paper container. Immediately thereafter it is admitted through a rectangular hole, $1\frac{1}{2}$ in.×$\frac{7}{8}$ in., in the lead housing. After traversing the cloud chamber, the beam leaves by way of a 4 in.×4 in. hole in the rear end of the lead housing and is stopped in a beam catcher.

IV. THE SHIELDING OF THE CHAMBER

The chamber rests on a layer of lead bricks 2 inches thick, which in turn rests on an ordinary concrete base 32 inches high. The rest of the shielding all around the chamber is built of lead bricks. The wall is 12 inches thick on the front side (toward the reactor) and 8 inches thick on the other three sides. From above, the chamber is shielded by a steel plate 1 inch thick which supports two layers of lead bricks for a total thickness of 4 inches of lead. Only in a small area just above the camera is the shielding reduced to $\frac{1}{2}$ inch of steel and 2 inches of lead. The outside dimensions of the lead housing are 28×52×48 in. In building up the shielding, care was taken to avoid any direct path from the room to the inside of the lead housing. Plastic bags filled with LiF powder have been put wherever possible, inside the Pb housing, around the chamber to decrease the number of radiative captures in the lead shielding. A lead wall 4 inches thick was also added between the main Pb housing and the mirror. It had surface dimensions of 32 in.×32 in. and a hole for the beam of size $5\frac{1}{2}$ in.×1 in. It was covered with Cd on the side facing the reactor.

With the reactor operating at 2 Mw, the gamma background outside the lead housing has been measured in different situations. With the beam gate closed, the gamma background is ~7 mr/hr between the pile face and the Pb wall. It is ~0.3 mr/hr between the Pb wall and the lead housing, and ranges between 0.3 and 1 mr/hr on the three other sides of the housing. When the neutron beam is on, the background goes to ~18 mr/hr between the pile face and the Pb wall and does not change by more than a factor of ~1.5 anywhere else. With the reactor operating at 2 Mw, the gamma background in the chamber at various points off the beam was found to be in the range from ~0.03 mr/hr to ~0.08 mr/hr when the beam was on. These figures are intended to give only an order of magnitude. The general background inside the chamber was not bigger with the neutron beam on than it was when the neutron beam was cut off with a sheet of Cd at the pile face. In the beam, right at the center of the chamber, the background was ~0.4 mr/hr, both with the neutron beam on and with the beam cut off by Cd at the pile face.

V. REMARKS ON THE OPERATION OF THE CHAMBER

The operation of the chamber working in a normal room background was discussed elsewhere.[8,9] A few remarks have to be added concerning the operation of the chamber in the higher background at the reactor and, in particular, when the neutron beam crosses the sensitive region. Inside the lead housing, as already mentioned, the general background with the neutron beam on is in the range between 0.03 and 0.08 mr/hr,

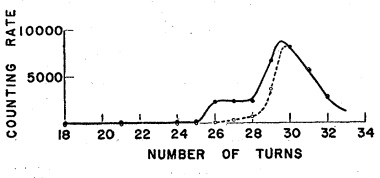

FIG. 5. Reflected beam at ~132 in. from the pile face. The mirror is tilted slightly less than in Fig. 4. The dotted line shows the effect of the lead plate used to cut off the gamma rays remaining at the very tail of the direct beam.

[9] G. Caglioti and N. D'Angelo, Rev. Sci. Instr. 28, 841 (1957).

i.e., it is several times the normal cosmic-ray background at sea level. To have the chamber working properly under such conditions, it was found not only desirable but necessary to have an electric sweeping field on at all times, with a voltage drop $\geqslant 20$–30 volts between the top and the bottom of the chamber, the top being negative. The same voltage drop, with the top of the chamber positive, did not provide satisfactory operation. A possible explanation of this fact was given elsewhere.[10] The voltage drop which was actually chosen was around 120–150 volts (top negative).

When the neutron mean is stopped at the pile face with a Cd sheet and only gamma rays are allowed to cross the chamber, one might notice a small increase in the background of the electrons originating in the sensitive region compared to what one can see when the beam gate is closed. A few electron tracks starting from the first Mylar window of the polystyrene cylinder cross the sensitive region also. When the neutron beam is on, one does not notice any increase of the electron background but a few short and heavy tracks appear. With the chamber working with a mixture of CO_2 ($\sim$5 psi) and helium ($\sim$25 psi), the number of heavy tracks observed in the sensitive region was fairly high (5–10 at any time). The vapor depletion produced by such heavy tracks could interfere very seriously with the observation of electron tracks in the region traversed by the beam. Hence their number had to be reduced. When the chamber was operated with oxygen alone at slightly above atmospheric pressure, the neutron beam produced no heavy tracks and the performance of the chamber was fairly satisfactory. This seemed to indicate that the heavy tracks observed when using the mixture of CO_2 and helium probably resulted from (n,p) reactions with He^3. Oxygen at $\sim$1 atmosphere did not provide a sensitive layer as deep as with the mixture of helium and CO_2.[11] Moreover, to prevent any nitrogen from entering the chamber, it was desirable to work at pressures slightly above atmospheric. A mixture of oxygen ($\sim\frac{1}{2}$ atmos) and helium ($\sim\frac{1}{2}$ atmos) was then chosen. The number of proton tracks still remaining was then too small to interfere with the observation of the electron tracks but still big enough to be used to locate the beam in the pictures, as will be seen in Sec. VI. Before filling with the above mixture, the chamber was usually flushed many times with oxygen to reduce possible traces of nitrogen.

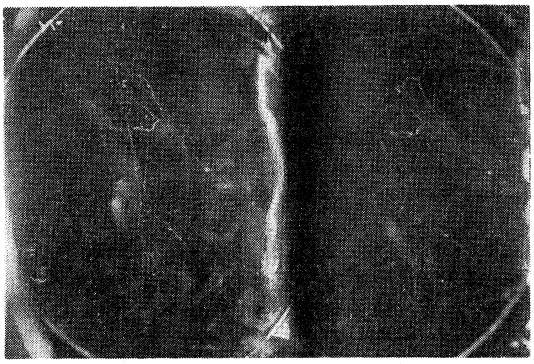

FIG. 6. Tracks observed with the chamber working with methyl alcohol diffusing in the mixture of oxygen and helium. The neutron beam is cut off with Cd at the pile face.

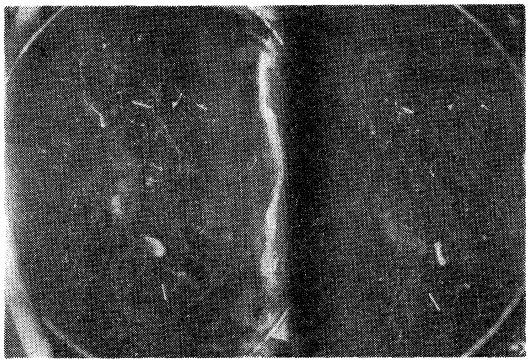

FIG. 7. Tracks observed with the chamber working with methyl alcohol diffusing in the mixture of oxygen and helium. The neutron beam is on. Note the short, heavy proton tracks.

Figures 6 and 7 are two pictures taken with the chamber working by diffusion of methyl alcohol in oxygen and helium, with a voltage drop of $\sim$150 volts between top and bottom of the chamber (top negative). The first picture was taken with the neutron beam stopped by a Cd sheet at the pile face. The second picture is intended to give an idea of the behavior of the chamber when the neutron beam is on.

VI. EXPERIMENTAL RESULTS

With the reactor operating at 2 Mw and the neutron beam on, pictures were taken of the events occurring in the chamber. These pictures were then projected on a screen where, for convenience in measuring, the tracks appeared slightly larger than their natural size. To locate the beam in the chamber, the proton tracks from the (n,p) reactions were used. In Fig. 8 are plotted the distributions of the end points of the proton tracks for the left and for the right side of the stereopictures. The dotted lines show the positions of the centers of the distributions. In Fig. 9 is a plot of the distribution of the distances between corresponding end points of the proton tracks in the two sides of the stereopictures, greater separations corresponding to end points nearer the bottom of the chamber. It should be noted that the nuclear reaction [$He^3(n,p)H^3$ or, less often $N^{14}(n,p)C^{14}$] responsible for a given track occurs at the "break" between the proton track and that of the residual nucleus—not at either end of the track.[12] Since the pressure in the chamber is not low enough to allow one

[10] N. D'Angelo, Rev. Sci. Instr. **29**, 433 (1958).
[11] Argan, D'Angelo, and Gigli, Nuovo cimento **10**, 1337 (1956).
[12] D. J. Hughes and C. Eggler, Phys. Rev. **73**, 809 (1948).

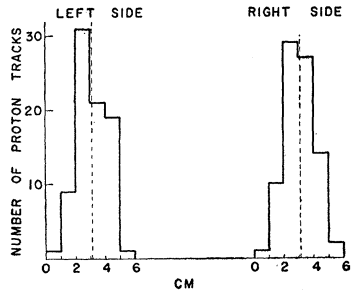

FIG. 8. Horizontal distribution of proton tracks on the projection plane.

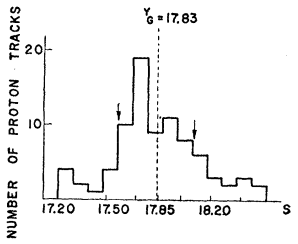

FIG. 9. Distribution of proton tracks as a function of the separation S in the projection plane. This separation measures the height of the track above the bottom of the chamber.

to locate this "break," the point at which the reaction occurs is uncertain. However, this circumstance does not affect the results of the measurements described below.

On the basis of the preliminary measurements on proton tracks, the following procedure was used for the selection of the electron tracks. Two rectangular strips each 2 cm wide and 22 cm long, were drawn on the projector plane, centered around the centers of the proton distributions. An electron track was accepted only if it had an end point in each strip. If this condition was met, then the separation was measured between the left and the right end points in the projector plane. If an electron track had two end points in both strips, both end points were considered. The distribution of the separations S of corresponding end points of electron tracks in the two sides of the pictures is shown in Fig. 10. A peak is evident around $S \approx 17.85$ cm, i.e., in the same position as for the proton tracks.

The same kind of measurement was made on the frames with the neutron beam stopped either with a Cd sheet at the pile face or with a plastic bag filled with loose LiF powder (3 or 4 cm thick) placed just before the first Mylar window of the cloud chamber. In both cases the peak around $S \approx 17.85$ cm disappeared. The

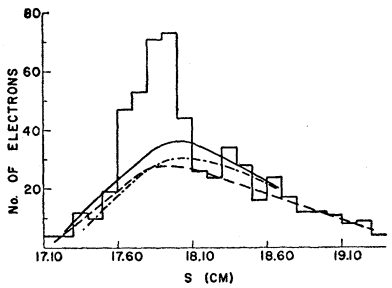

FIG. 10 Electron distribution with the neutron beam on. The separation S measures the height above the bottom of the chamber.

combined results of the two methods of stopping the beam is plotted in Fig. 11. As an additional check, the same kind of vertical scanning of the electron tracks was repeated when the rectangular strips (2 cm wide and 16 cm long in the projection plane) were displaced about 2 cm off the neutron beam. In this case also, no peak is evident around $S \approx 17.85$ cm (Fig. 12). In each of the three series of scannings, the two strips in the projector plane were divided in two equal parts by a line normal to the beam and a count was made of the number of accepted end points of electron tracks in each half. The end points turned out to be divided equally between the two regions, within the statistical fluctuations, as it should be if the chamber was working properly and no troubles such as nonuniform illumination of the sensitive region were present.

The above results seem to be a fairly strong proof that the observed peak around $S \approx 17.85$ cm in Fig. 10 is associated with the decay of neutrons. Actually two other mechanisms of production of that peak could be considered: (*a*) short-lived beta activation of the filling mixture in the region traversed by the beam, or (*b*)

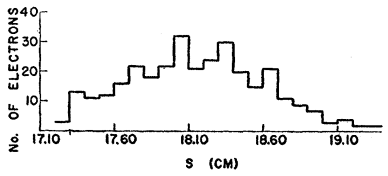

FIG. 11. Electron distribution like that in Fig. 10 except that the neutron beam is cut off.

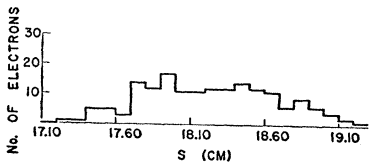

FIG. 12. Electron distribution like that in Fig. 10 except it is taken to one side of the neutron beam.

internal conversions following neutron captures in the filling mixture along the beam. As for (*a*), no such short half-lives associated with capture cross sections big enough to produce the observed effects are known for the elements presumed to be present in the chamber. As for (*b*), the order of magnitude of the effect in the gases used to fill the chamber is too small to give any appreciable contribution to the peak around $S = 17.85$ cm. When this is combined with the facts that neutron decay has indeed been observed in vacuum and that the half-life determined in that way coincides with the present determination, it is apparent that (*a*) and (*b*) are ruled out.

The neutron density in the chamber was measured by activation of gold foils. The horizontal distribution of the neutron density along an axis perpendicular to the beam is plotted in Fig. 13. The central region between the two vertical lines corresponds to the two rectangular strips in the projector plane used in the scanning of the electron tracks. The activation of the thin ($\sim$1 mil) gold foils exposed in the beam was compared with the

activation of a similar gold foil exposed in a standard pile. Corrections were made for the presence of "epicadmium" neutrons and the depression which the foil produced in the neutron density in the standard pile.[13,14] A large fraction of the correction for "epicadmium" neutrons seemed to be due to the large resonance in gold at 4.9 ev. This was proved by irradiating, in the same slot of the standard pile, a sandwich of five gold foils of equal size (1 cm×1 cm and ~1 mil thick). Their activities, reduced to equal weights of the foils, are plotted in Fig. 14. The difference in the counting rates for the central foil (No. 3) and the upper foil (No. 1) of the set is of the order of 7%. It can be easily shown that the mean life τ for the neutron decay is given by

$$\tau=-\frac{l}{q}\frac{\Phi}{\bar{v}}\left[\frac{e^{-\lambda t}(e^{\lambda t_f}-1)}{A(t)}\right]_{\text{calibr}}\left[\sum_t \frac{A(t)}{e^{-\lambda t}(e^{\lambda t_f}-1)}\right]_{\text{beam}} f,$$

where l is the length of the region along the beam where the decays are observed, q is the number of decays per min, $\Phi/\bar{v}$ is the density of slow neutrons in the standard pile, $A(t)$ is the counting rate (corrected for weight, counter efficiency, background, etc.) of the gold foils,

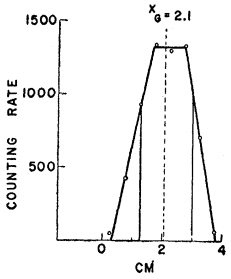

FIG. 13. Horizontal distribution of the neutron density in the cloud chamber.

t_f is the irradiation time, t the time since the beginning of the irradiation, f is the fraction of the total neutron flux responsible for the decays observed in the two rectangular strips of the projector plane, and the subscripts "beam" and "calibr" indicate that the brackets are to be evaluated for exposure in the beam and in the standard pile, respectively.

The counting rate of the gold foil used for calibration (corrected for weight, background, counter efficiency, epicadmium neutrons, and flux depression) turned out to be 115 counts/min in the standard counter. The corresponding t and t_f were $t=4058$ min and $t_f=4050$ min. For the sample in the beam, the quantity $\sum A(t)/[e^{-\lambda t}(e^{\lambda t_f}-1)]$ turned out to be 5.35×10^4 counts/min when the corrections for the weight of the foils, background, and counter efficiency were applied; Φ was 4500 neutrons cm^{-2} sec^{-1}, $\bar{v}$ was taken as 2.20×10^5 cm/sec, l was 19.0 cm, and f was 0.731. Hence $\tau=67.84/q$ and will be in minutes if q is given in min^{-1}. It was found that $q=3.69$ electrons/min so $\tau=18.33$ min. The

[13] D. J. Hughes, *Pile Neutron Research* (Addison-Wesley Publishing Company, Inc., Reading, Massachusetts, 1953).
[14] E. D. Klema and R. H. Ritchie, Phys. Rev. **87**, 167 (1952).

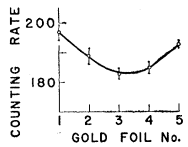

FIG. 14. Effect of the gold resonance of 4.9 ev.

half-life is then $0.693\tau=12.7$ min. The accuracy to which the flux in the standard pile is known is about 5%. When this is combined with the errors introduced in comparing the flux in the standard pile and the flux in the neutron beam, an over-all error of ~7% might result in the flux measurement.

Another source of error could be that the two strips in the projector plane (used for the scanning) might have been displaced from the real position of the neutron beam. This error is small compared with the one above.

The flux fluctuations caused by the oscillations in the reactor were checked with the counter used to map the beam. They are believed to be less than 1%.

The possibility of missing a good event in scanning the film seems to be very small indeed. With the film rate of 2 frames/sec, a track born ~1 inch from the bottom of the chamber is visible for at least three frames. It could escape detection only if missed all three times.

Some uncertainty could arise in measuring the point of origin of an electron track. This possibility was checked by scanning the same roll of film at two different times about 3 weeks apart. Essentially the same results were obtained from the two scannings.

To subtract the background from the peak produced by neutron decays, the number of electron end points was plotted against S for each of the three runs shown in Figs. 10, 11, and 12. respectively, and normalized to the data of Fig. 10. The background with the neutron beam cut off by Cd or LiF is slightly bigger than in the two other cases. This is probably a result of the gamma rays produced by neutron captures in the Cd sheet at the pile face. In the other two instances the backgrounds are essentially the same. The last two have been assumed to give the right background in the peak

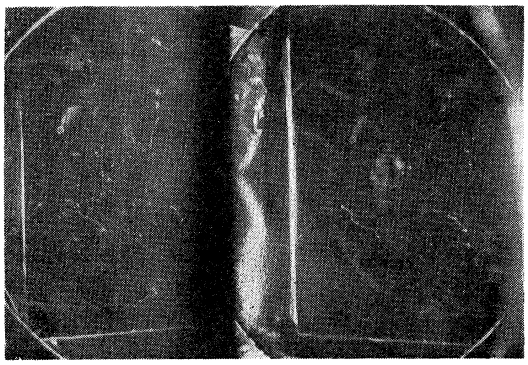

FIG. 15. Stereo picture of an electron track showing a kind of cluster which could be attributed to the decay proton.

region. The statistical errors in counting the electron tracks amount to ~10%, when the subtraction of the background is taken into account.

The over-all uncertainty in the half-life given by the present measurement is thus believed to be ~15%.

It probably should be added that a very small fraction of the electron tracks starting from the neutron beam seemed to have a kind of cluster at the point of origin (Fig. 15). Although this could possibly be attributed to the decay proton, it must be emphasized that the measurements described above give no evidence for this.

VII. CONCLUSIONS

The cloud chamber method of measuring the half-life of the free neutron proved successful. The main sources of error seem to be in the flux measurement and in the poor statistics. If the statistical error can be reduced to ~3% and the error in the flux measurement to something like 3–4%, an over-all error of about 6–7% should result.

Although the present determination has not improved on the best previous measurement of the half-life of the neutron, it has about equal accuracy and confirms it by an independent method.

ACKNOWLEDGMENTS

G. Caglioti shared in the early stages of this experiment and his help and contributions are very gratefully acknowledged. It is a pleasure to thank E. Hupke for the considerable assistance rendered at several phases of the work.

PHYSICAL REVIEW VOLUME 114, NUMBER 1 APRIL 1, 1959

Nuclear Structure Effects in Internal Conversion Coefficients by Configuration Mixing*

L. S. KISSLINGER†
Western Reserve University, Cleveland, Ohio, and Oak Ridge National Laboratory, Oak Ridge, Tennessee
(Received June 2, 1958)

The nuclear matrix elements which are needed to determine the internal conversion coefficients when a finite nucleus is employed are derived for nuclei for which the shell model wave functions are a good zero-order approximation for low-energy processes. Using configuration mixing, general expressions are derived for these matrix elements. It is shown that the nuclear structure alteration can be ten to twenty percent or more for l-forbidden transitions. Numerical results are given for the $M1$ and $E2$ 279-kev transitions in Tl^{203}.

I. INTRODUCTION

THE internal conversion coefficients convey important information about the atomic nucleus. The point nucleus calculations of the internal conversion coefficients[1] have been extremely valuable in determining the angular momentum and parity of nuclei. However, for large values of the atomic number, Z, corrections must be made for the extended nucleus. Sliv *et al.*[2] have calculated the alteration in the coefficients when the electron wave functions calculated for an extended, rather than a point nucleus, are used, i.e., the static effect. More recently, the conversion coefficients with the static effect included also have been calculated by Rose.[3] But without rather unphysical assumptions about the nuclear currents, the calculation of the internal conversion coefficients for a finite nuclear size requires the knowledge of the nuclear wave functions in order to calculate certain nuclear matrix elements (or the demonstration that they are unimportant).[4]

This dependence of the conversion coefficients on the nuclear wave functions makes the use of the experimental results less straightforward for determining nuclear properties. However, it has the advantage that an accurate measurement of the coefficients can give additional information about the details of nuclear structure. In particular, conversion coefficients can now help to provide information about the accuracy of nuclear models.

In the original work of Church and Weneser and in the more recent work of Green and Rose[5] the internal conversion coefficients are given by the power series expressions which separate the alterations which proceed

* This research was supported in part by the Oak Ridge Institute of Nuclear Studies and in part by the U. S. Air Force through the Air Force Office of Scientific Research of the Air Research and Development Command. For a more detailed treatment of this work see the Oak Ridge National Laboratory Report ORNL-2556 (unpublished).

† Oak Ridge Institute of Nuclear Studies Summer Research Participant, 1957.

[1] Rose, Goertzel, Spinrad, Harr, and Strong, Phys. Rev. **76**, 1883 (1949); and unpublished tables by M. E. Rose *et al.*

[2] L. A. Sliv and I. M. Band, Leningrad Physico-Technical Institute Reports 1956 and 1958 [translation: Reports 57ICCK1 and 58ICCL1, issued by Physics Department, University of Illinois, Urbana, Illinois (unpublished)].

[3] M. E. Rose, *Internal Conversion Coefficients* (North-Holland Publishing Company, Amsterdam, 1958).

[4] E. L. Church and J. Weneser, Phys. Rev. **104**, 1382 (1956).

[5] T. A. Green and M. E. Rose, Oak Ridge National Laboratory Report ORNL-2395 (unpublished); Phys. Rev. **110**, 105 (1958).

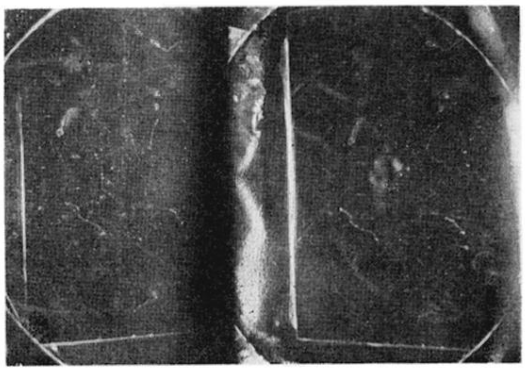

FIG. 15. Stereo picture of an electron track showing a kind of cluster which could be attributed to the decay proton.

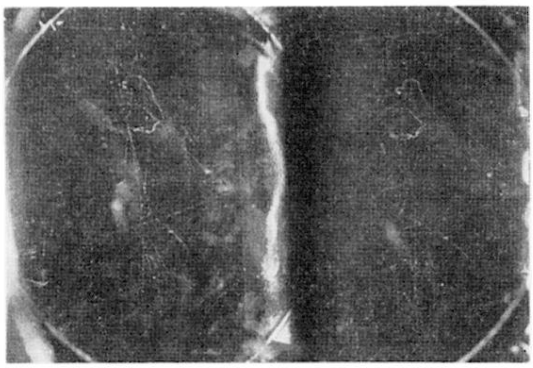

FIG. 6. Tracks observed with the chamber working with methyl alcohol diffusing in the mixture of oxygen and helium. The neutron beam is cut off with Cd at the pile face.

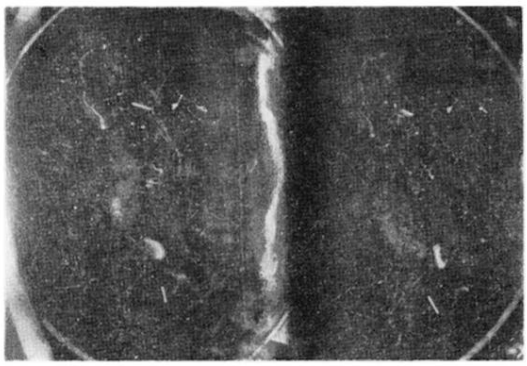

FIG. 7. Tracks observed with the chamber working with methyl alcohol diffusing in the mixture of oxygen and helium. The neutron beam is on. Note the short, heavy proton tracks.